2012

Energy dissipation and switching delay in stress-induced switching of multiferroic nanomagnets in the presence of thermal fluctuations

Kuntal Roy
Virginia Commonwealth University, royk@vcu.edu

Supriyo Bandyopadhyay
Virginia Commonwealth University, sbandy@vcu.edu

Jayasimha Atulasimha
Virginia Commonwealth University, jatulasimha@vcu.edu

Roy, K., Bandyopadhyay, S., & Atulasimha, J. Energy dissipation and switching delay in stress-induced switching of multiferroic nanomagnets in the presence of thermal fluctuations. Journal of Applied Physics, 112, 023914 (2012).

Energy dissipation and switching delay in stress-induced switching of multiferroic nanomagnets in the presence of thermal fluctuations

Kuntal Roy,[1,a)] Supriyo Bandyopadhyay,[1] and Jayasimha Atulasimha[2]
[1]*Department of Electrical and Computer Engineering, Virginia Commonwealth University, Richmond, Virginia 23284, USA*
[2]*Department of Mechanical and Nuclear Engineering, Virginia Commonwealth University, Richmond, Virginia 23284, USA*

(Received 25 November 2011; accepted 2 July 2012; published online 25 July 2012)

Switching the magnetization of a shape-anisotropic 2-phase multiferroic nanomagnet with voltage-generated stress is known to dissipate very little energy (<1 aJ for a switching time of ~0.5 ns) at 0 K temperature. Here, we show by solving the stochastic Landau-Lifshitz-Gilbert equation that switching can be carried out with ~100% probability in less than 1 ns while dissipating less than 1.5 aJ at *room temperature*. This makes nanomagnetic logic and memory systems, predicated on stress-induced magnetic reversal, one of the most energy-efficient computing hardware extant. We also study the dependence of energy dissipation, switching delay, and the critical stress needed to switch, on the rate at which stress on the nanomagnet is ramped up or down. © *2012 American Institute of Physics*. [http://dx.doi.org/10.1063/1.4737792]

I. INTRODUCTION

Shape-anisotropic multiferroic nanomagnets, consisting of magnetostrictive layers elastically coupled with piezoelectric layers,[1–5] have emerged as attractive storage and switching elements for non-volatile memory and logic systems since they are potentially very energy-efficient. Their magnetizations can be switched in less than 1 nanosecond with energy dissipation less than 1 aJ, when no thermal noise is present[6,7] This has led to multiple logic proposals incorporating these systems.[8–10] The magnetization of the magnet has two (mutually anti-parallel) stable states along the easy axis that encode the binary bits 0 and 1. The magnetization is flipped from one stable state to the other by applying a tiny voltage of few tens of millivolts across the piezoelectric layer while constraining it from expanding or contracting along its in-plane hard-axis (see Fig. 1). The voltage generates a strain in the piezoelectric layer, which is then transferred to the magnetostrictive layer. This produces a uniaxial stress in the magnetostrictive layer along its easy-axis and rotates the magnetization towards the in-plane hard axis as long as the product of the stress and the magnetostrictive coefficient is *negative*. By convention, a tensile stress is positive and a compressive stress is negative. There have been experimental efforts to demonstrate such electric-field induced magnetization rotation both in multi-domain[11] and single-domain nanomagnets.[12–14]

In this paper, we have studied the switching dynamics of a single-domain magnetostrictive nanomagnet, subjected to uniaxial stress, in the presence of thermal fluctuations. The dynamics is governed by the stochastic Landau-Lifshitz-Gilbert (LLG) equation[15,16] that describes the time-evolution of the magnetization vector's orientation under various torques. There are *three* torques to consider here: the torque due to shape anisotropy, the torque due to stress, and the torque associated with random thermal fluctuations. With experimentally feasible ramp rates (rate at which stress on the magnet is ramped up or down), a magnet can be switched with ~100% probability with a (thermally averaged) switching delay of ~0.5 ns and (thermally averaged) energy dissipation ~200 kT at room-temperature. This is very promising for "beyond-Moore's law" ultra-low-energy computing.[17–19] Our simulation results show the following: (1) a fast ramp and a sufficiently high stress are required to switch the magnet with high probability in the presence of thermal noise, (2) the stress needed to switch with a given probability increases with decreasing ramp rate, (3) if the ramp rate is too slow, then the switching probability may never approach 100% no matter how much stress is applied, (4) the switching probability increases monotonically with stress and saturates at ~100% when the ramp is fast, but exhibits a non-monotonic dependence on stress when the ramp is slow, and (5) the thermal averages of the switching delay and energy dissipation are nearly independent of the ramp rate if we always switch with the critical stress, which is the minimum value of stress needed to switch with non-zero probability in the presence of noise.

II. MODEL

A. Magnetization dynamics of a magnetostrictive nanomagnet in the presence of thermal noise: Solution of the stochastic Landau-Lifshitz-Gilbert equation

Consider an isolated nanomagnet in the shape of an elliptical cylinder whose elliptical cross section lies in the y-z plane with its major axis aligned along the z-direction and minor axis along the y-direction (see Fig. 1). The dimension of the major axis is a, that of the minor axis is b, and the thickness is l. The magnet's volume is $\Omega = (\pi/4)abl$. The z-axis is the easy axis, the y-axis is the in-plane hard axis and the x-axis is the out-of-plane hard axis. Since $l \ll b$, the

a)Electronic mail: royk@vcu.edu.

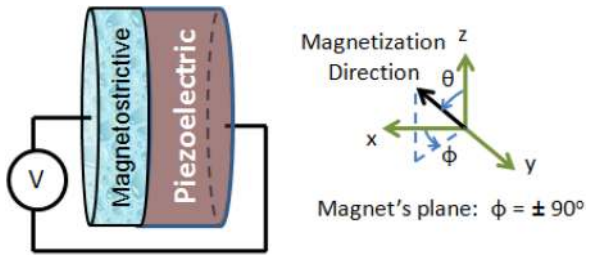

FIG. 1. A two-phase multiferroic nanomagnet in the shape of an elliptical cylinder is stressed with an applied voltage via the d_{31} coupling in the piezoelectric. The multiferroic is prevented from expanding or contracting along the in-plane hard axis (y-axis), so that a uniaxial stress is generated along the easy axis (z-axis).

out-of-plane hard axis is much harder than the in-plane hard axis. Let $\theta(t)$ be the polar angle and $\phi(t)$ the azimuthal angle of the magnetization vector.

The total energy of the single-domain, magnetostrictive, polycrystalline nanomagnet, subjected to uniaxial stress along the easy axis (major axis of the ellipse) is the sum of the uniaxial shape anisotropy energy and the uniaxial stress anisotropy energy.[20] The former is given by[20] $E_{SHA}(t) = (\mu_0/2)M_s^2\Omega N_d(t)$, where M_s is the saturation magnetization and $N_d(t)$ is the demagnetization factor expressed as[20]

$$N_d(t) = N_{d-zz}\cos^2\theta(t) + N_{d-yy}\sin^2\theta(t)\sin^2\phi(t) + N_{d-xx}\sin^2\theta(t)\cos^2\phi(t), \quad (1)$$

with N_{d-zz}, N_{d-yy}, and N_{d-xx} being the components of the demagnetization factor along the z-axis, y-axis, and x-axis, respectively.[21] These factors depend on the dimensions of the magnet (values of a, b, and l). We choose these dimensions as $a = 100$ nm, $b = 90$ nm, and $l = 6$ nm, which ensures that the magnet has a single ferromagnetic domain.[22] These dimensions also determine the shape anisotropy energy barriers. The in-plane barrier E_b, which is the difference between the shape anisotropy energies when $\theta = 90^\circ$ and $\theta = 0^\circ, 180^\circ$ ($\phi = \pm 90^\circ$) determines the static error probability, which is the probability of spontaneous magnetization reversal due to thermal noise. This probability is $\exp[-E_b/kT]$. For the dimensions and material chosen, $E_b = 44$ kT at room temperature, so that the static error probability at room temperature is e^{-44}.

The stress anisotropy energy is given by[20] $E_{STA}(t) = -(3/2)\lambda_s\sigma(t)\Omega\cos^2\theta(t)$, where $(3/2)\lambda_s$ is the magnetostriction coefficient of the nanomagnet and $\sigma(t)$ is the stress at an instant of time t. Note that a positive $\lambda_s\sigma(t)$ product will favor alignment of the magnetization along the major axis (z-axis), while a negative $\lambda_s\sigma(t)$ product will favor alignment along the minor axis (y-axis), because that will minimize $E_{STA}(t)$. In our convention, a compressive stress is negative and tensile stress is positive. Therefore, in a material like Terfenol-D that has positive λ_s, a compressive stress will favor alignment along the minor axis (in-plane hard axis) and tensile along the major axis (easy axis).[6]

At any instant of time t, the total energy of the nanomagnet can be expressed as

$$E(t) = E(\theta(t), \phi(t), \sigma(t)) = B(t)\sin^2\theta(t) + C(t), \quad (2)$$

where

$$B(t) = B_0(t) + B_{stress}(t), \quad (3a)$$

$$B_0(t) = (\mu_0/2)M_s^2\Omega[N_{d-xx}\cos^2\phi(t) + N_{d-yy}\sin^2\phi(t) - N_{d-zz}], \quad (3b)$$

$$B_{stress}(t) = (3/2)\lambda_s\sigma(t)\Omega, \quad (3c)$$

$$C(t) = (\mu_0/2)M_s^2\Omega N_{d-zz} - (3/2)\lambda_s\sigma(t)\Omega. \quad (3d)$$

The torque acting on the magnetization per unit volume due to shape and stress anisotropy is

$$\mathbf{T_E}(t) = -\mathbf{n_m}(t) \times \nabla E(\theta(t), \phi(t), \sigma(t)) = -2B(t)\sin\theta(t)\cos\theta(t)\,\hat{\mathbf{e}}_\phi - B_{0e}(t)\sin\theta(t)\,\hat{\mathbf{e}}_\theta, \quad (4)$$

where $B_{0e}(t) = (\mu_0/2)\,M_s^2\Omega(N_{d-xx} - N_{d-yy})\sin(2\phi(t))$.

The torque due to thermal fluctuations is treated via a random magnetic field $\mathbf{h}(t)$ and is expressed as

$$\mathbf{h}(t) = h_x(t)\hat{\mathbf{e}}_\mathbf{x} + h_y(t)\hat{\mathbf{e}}_\mathbf{y} + h_z(t)\hat{\mathbf{e}}_\mathbf{z}, \quad (5)$$

where $h_x(t)$, $h_y(t)$, and $h_z(t)$ are the three components of the random thermal field $\mathbf{h}(t)$ in x-, y-, and z-directions, respectively, in Cartesian coordinates. We assume the properties of the random field $\mathbf{h}(t)$ as described in Ref. 16. Accordingly, the random thermal field can be expressed as[19]

$$h_i(t) = \sqrt{\frac{2\alpha kT}{|\gamma|(1+\alpha^2)M_V\Delta t}}\,G_{(0,1)}(t) \qquad (i = x, y, z), \quad (6)$$

where α is the dimensionless phenomenological Gilbert damping constant, $\gamma = 2\mu_B\mu_0/\hbar$ is the gyromagnetic ratio for electrons and is equal to 2.21×10^5 (rad · m) · (A · s)$^{-1}$, μ_B is the Bohr magneton, $M_V = \mu_0 M_s\Omega$, and $1/\Delta t$ is proportional to the attempt frequency of the thermal field. Consequently, Δt should be the simulation time-step used to simulate switching trajectories in the presence of random thermal torque. The quantity $G_{(0,1)}(t)$ is a Gaussian distribution with zero mean and unit variance.[23]

The thermal torque can be written as

$$\mathbf{T_{TH}}(t) = M_V\,\mathbf{n_m}(t) \times \mathbf{h}(t) = P_\theta(t)\,\hat{\mathbf{e}}_\phi - P_\phi(t)\,\hat{\mathbf{e}}_\theta, \quad (7)$$

where

$$P_\theta(t) = M_V[h_x(t)\cos\theta(t)\cos\phi(t) + h_y(t)\cos\theta(t)\sin\phi(t) - h_z(t)\sin\theta(t)] \quad (8)$$

$$P_\phi(t) = M_V[h_y(t)\cos\phi(t) - h_x(t)\sin\phi(t)]. \quad (9)$$

The magnetization dynamics under the action of the torques $\mathbf{T_E}(t)$ and $\mathbf{T_{TH}}(t)$ is described by the stochastic LLG equation as follows:

$$\frac{d\mathbf{n_m}(t)}{dt} - \alpha\left(\mathbf{n_m}(t) \times \frac{d\mathbf{n_m}(t)}{dt}\right) = -\frac{|\gamma|}{M_V}[\mathbf{T_E}(t) + \mathbf{T_{TH}}(t)]. \quad (10)$$

From the last equation, we get the following coupled equations for the dynamics of $\theta(t)$ and $\phi(t)$:

$$(1+\alpha^2)\frac{d\theta(t)}{dt} = \frac{|\gamma|}{M_V}[B_{0e}(t)\sin\theta(t) - 2\alpha B(t)\sin\theta(t)\cos\theta(t) + (\alpha P_{\theta(t)} + P_{\phi(t)})]. \tag{11}$$

$$(1+\alpha^2)\frac{d\phi(t)}{dt} = \frac{|\gamma|}{M_V}[\alpha B_{0e}(t) + 2B(t)\cos\theta(t) - [\sin\theta(t)]^{-1}(P_{\theta(t)} - \alpha P_{\phi(t)})]. \quad (\sin\theta \neq 0.) \tag{12}$$

These equations describe the magnetization dynamics, namely the temporal evolution of the magnetization vector's orientation, in the presence of thermal noise.

B. Fluctuation of magnetization around the easy axis (stable orientation) due to thermal noise

The torque on the magnetization vector due to shape and stress anisotropy vanishes when $\sin\theta = 0$ [see Eq. (4)], i.e., when the magnetization vector is aligned along the easy axis. That is why $\theta = 0^\circ, 180^\circ$ are called *stagnation points*. Only thermal fluctuations can budge the magnetization vector from the easy axis. To see this, consider the situation when $\theta = 180^\circ$. We get

$$\phi(t) = \tan^{-1}\left(\frac{\alpha h_y(t) + h_x(t)}{h_y(t) - \alpha h_x(t)}\right), \tag{13}$$

$$\theta'(t) = -|\gamma|\frac{h_x^2(t) + h_y^2(t)}{\sqrt{(h_y(t) - \alpha h_x(t))^2 + (\alpha h_y(t) + h_x(t))^2}}. \tag{14}$$

We can see clearly from the above equation that thermal torque can deflect the magnetization from the easy axis since the time rate of change of $\theta(t)$ [i.e., $\theta'(t)$] is non-zero in the presence of the thermal field. Note that the initial deflection from the easy axis due to the thermal torque does not depend on the component of the random thermal field along the z-axis, i.e., $h_z(t)$, which is a consequence of having $\pm z$-axis as the easy axes of the nanomagnet. However, once the magnetization direction is even slightly deflected from the easy axis, all three components of the random thermal field along the x-, y-, and z-directions would come into play and affect the deflection.

C. Thermal distribution of the initial orientation of the magnetization vector

The thermal distributions of θ and ϕ in the unstressed magnet are found by solving the Eqs. (11) and (12) while setting $B_{stress} = 0$. This will yield the distribution of the magnetization vector's initial orientation when stress is turned on. The θ-distribution is Boltzmann peaked at $\theta = 0^\circ$ or 180°, while the ϕ-distribution is Gaussian peaked at $\phi = \pm 90^\circ$ (Ref. 24). Since the most probable value of θ is either 0° or 180°, where stress is ineffective (*stagnation point*), there are long tails in the switching delay distribution at any temperature. They are due to the fact that when we start out from $\theta = 0^\circ, 180^\circ$, we have to wait a while before thermal kick sets the switching in motion. Thus, switching trajectories initiating from a stagnation point are very slow.[25,26]

In order to eliminate the long tails in the switching delay distribution and thus decrease the mean switching delay, one can apply a small static bias magnetic field that will shift the peak of $\theta_{initial}$ distribution away from the easy axis, so that the most probable starting orientation will no longer be a stagnation point. This field is applied along the out-of-plane hard axis ($+x$-direction) so that the potential energy due to the applied magnetic field becomes $E_{mag}(t) = -M_V H \sin\theta(t)\cos\phi(t)$, where H is the magnitude of magnetic field. The torque generated due to this field is $\mathbf{T_M}(t) = -\mathbf{n_m}(t) \times \nabla E_{mag}(\theta(t), \phi(t))$. The presence of this field will modify Eqs. (11) and (12) to

$$(1+\alpha^2)\frac{d\theta(t)}{dt} = \frac{|\gamma|}{M_V}[B_{0e}(t)\sin\theta(t) - 2\alpha B(t)\sin\theta(t)\cos\theta(t) + \alpha M_V H\cos\theta(t)\cos\phi(t) - M_V H\sin\phi(t) + (\alpha P_{\theta(t)} + P_{\phi(t)})], \tag{15}$$

$$(1+\alpha^2)\frac{d\phi(t)}{dt} = \frac{|\gamma|}{M_V}[\alpha B_{0e}(t) + 2B(t)\cos\theta(t) - [\sin\theta(t)]^{-1}\left(M_V H\cos\theta(t)\cos\phi(t) + \alpha M_V H\sin\phi(t)\right) - [\sin\theta(t)]^{-1} \times (P_{\theta(t)} - \alpha P_{\phi(t)})]. \quad (\sin\theta \neq 0.) \tag{16}$$

The bias field also makes the potential energy profile of the magnet asymmetric in ϕ-space and the energy minimum will be shifted from $\phi_{min} = \pm 90^\circ$ (the plane of the magnet) to

$$\phi_{min} = \cos^{-1}\left[\frac{H}{M_s(N_{d-xx} - N_{d-yy})}\right]. \tag{17}$$

However, the potential profile will remain symmetric in θ-space, with $\theta = 0^\circ$ and $\theta = 180^\circ$ remaining as the minimum energy locations. With the parameters used in this paper, a bias magnetic field of flux density 40 mT applied perpendicular to the plane of the magnet would make $\phi_{min} \simeq \pm 87^\circ$, i.e., deflect the magnetization vector $\sim 3^\circ$ from the magnet's plane. Application of the bias magnetic field will also reduce the in-plane shape anisotropy energy barrier from 44 kT to 36 kT at room temperature. We assume that a permanent magnet will be employed to produce the bias field and thus will not require any additional energy dissipation to be generated.

D. Energy dissipation

The energy dissipated during switching has two components: (1) the energy dissipated in the switching circuit that applies the stress on the nanomagnet by generating a voltage, and (2) the energy dissipated internally in the nanomagnet because of Gilbert damping. We will term the first component "CV^2" dissipation, where C and V denote the capacitance of the piezoelectric layer and the applied voltage,

respectively. If the voltage is turned on or off abruptly, i.e., the ramp rate is infinite, then the energy dissipated during either turn on or turn off is $(1/2)CV^2$. However, if the ramp rate is finite, then this energy is reduced and its exact value will depend on the ramp duration or ramp rate. We calculate it following the same procedure described in Ref. 7. The second component, which is the internal energy dissipation E_d, is given by the expression $\int_0^\tau P_d(t)dt$, where τ is the switching delay and $P_d(t)$ is the power dissipated during switching[27,28]

$$P_d(t) = \frac{\alpha|\gamma|}{(1+\alpha^2)M_V}|\mathbf{T_E}(t) + \mathbf{T_M}(t)|^2. \quad (18)$$

We sum up the power $P_d(t)$ dissipated during the entire switching period to get the corresponding energy dissipation E_d and add that to the "CV^2" dissipation in the switching circuit to find the total dissipation E_{total}. The average power dissipated during switching is simply E_d/τ.

There is no net dissipation due to random thermal torque, however, that does not mean that the temperature has no effect on either E_d or the "CV^2" dissipation. It affects E_d since it raises the critical stress needed to switch with $\sim$100% probability and it also affects the stress needed to switch with a given probability. Furthermore, it affects "CV^2" because V must exceed the thermal noise voltage[29] to prevent random switching due to noise. In other words, we must enforce $CV^2 > kT$. For the estimated capacitance of our structure (2.6 fF), this translates to $V > 1.3$ mV.

III. SIMULATION RESULTS AND DISCUSSIONS

In our simulations, we consider the magnetostrictive layer to be made of polycrystalline Terfenol-D that has the following material properties—Young's modulus (Y): 8×10^{10} Pa, magnetostrictive coefficient $((3/2)\lambda_s)$: $+90 \times 10^{-5}$, saturation magnetization (M_s): 8×10^5 A/m, and Gilbert's damping constant (α): 0.1 (Refs. 30–33). For the piezoelectric layer, we use lead-zirconate-titanate (PZT), which has a dielectric constant of 1000. The PZT layer is assumed to be four times thicker than the magnetostrictive layer so that any strain generated in it is transferred almost completely to the magnetostrictive layer.[6] The maximum strain that can be generated in the PZT layer is 500 ppm,[34,35] which would require a voltage of 66.7 mV because $d_{31} = 1.8 \times 10^{-10}$ m/V for PZT.[36] This strain is assumed to be transferred completely to the magnetostrictive layer, so the corresponding stress in Terfenol-D is the product of the generated strain (500×10^{-6}) and the Young's modulus (8×10^{10} Pa). Hence, 40 MPa is the maximum stress that can be generated in the Terfenol-D nanomagnet. The strain-voltage relationship in PZT is actually *superlinear* since d_{31} increases with electric field.[35] Hence, the voltage needed to produce 500 ppm strain in the Terfenol-D layer will be considerably *less* than 66.7 mV. Throughout this paper, we have assumed a linear strain-voltage relationship and assumed the low-field value of d_{31}. This will result in overestimation of the voltage needed to generate a given strain in the Terfenol-D layer and also overestimation of the energy dissipation. We did this to err on the side of caution; our energy dissipation estimates will be pessimistic rather than optimistic.

We assume that when a compressive stress is applied to initiate switching, the magnetization vector starts out from near the south pole ($\theta \simeq 180^\circ$) with a certain ($\theta_{initial}$, $\phi_{initial}$) picked from the initial angle distributions at the given temperature. Stress is ramped up linearly and kept constant until the magnetization reaches the plane defined by the in-plane and the out-of-plane hard axis (i.e., the $x-y$ plane, $\theta = 90^\circ$). This plane is always reached sooner or later since the energy minimum of the stressed magnet in θ-space is at $\theta = 90^\circ$. Thermal fluctuations can introduce a spread in the time it takes to reach the $x-y$ plane but cannot prevent the magnetization from reaching it ultimately if the stress is so large that the energy minimum at $\theta = 90^\circ$ is more than a few kT deep.

As soon as the magnetization reaches the $x-y$ plane, the stress is ramped down at the same rate at which it was ramped up, and reversed in magnitude to aid switching. The magnetization dynamics ensures that θ continues to rotate towards 0° with very high probability. When θ becomes $\leq 5^\circ$, switching is deemed to have completed. A moderately large number (10000) of simulations, with their corresponding ($\theta_{initial}$, $\phi_{initial}$) picked from the initial angle distributions, are performed for each value of stress and ramp duration to generate the simulation results in this paper.

Fig. 2 shows the distributions of initial angles $\theta_{initial}$ and $\phi_{initial}$ in the presence of thermal fluctuations and a bias magnetic field applied along the out-of-plane direction ($+x$-axis). The latter has shifted the peak of $\theta_{initial}$ from the easy axis ($\theta = 180^\circ$). In Fig. 2(b), the $\phi_{initial}$ distribution has two peaks and resides mostly within the interval $[-90^\circ, +90^\circ]$ since the bias magnetic field is applied in the $+x$-direction. Because the magnetization vector starts out from near the south pole ($\theta \simeq 180^\circ$) when stress is turned on, the effective torque on the magnetization $[-|\gamma|/(1+\alpha^2)\mathbf{M} \times \mathbf{H}$, where $\mathbf{M}$ is the magnetization and $\mathbf{H}$ is the effective field] due to the $+x$-directed magnetic field is such that the magnetization prefers the ϕ-quadrant (0°, 90°) slightly over the ϕ-quadrant (270°, 360°), which is the reason for the asymmetry in the two distributions of $\phi_{initial}$. Consequently, when the magnetization vector starts out from $\theta \simeq 180^\circ$, the initial azimuthal angle $\phi_{initial}$ is more likely to be in the quadrant (0°, 90°) than the quadrant (270°, 360°).

Fig. 3 shows the switching probability as a function of stress for different ramp durations (60 ps, 90 ps, 120 ps)[7,37] at room temperature (300 K). We assume that the voltage generating the stress in PZT is applied from a voltage source with the PZT layer acting as a capacitance. The access resistance to the layer (through metallic wires) cannot exceed 500 Ω, and the capacitance of the PZT layer is $\sim$2 fF. Hence, the switching circuit is a simple series resistance-capacitance (RC) circuit with a time constant of no more than 1 ps, which makes the assumed ramp durations of 60/90/120 ps very reasonable. Since ferroelectrics can be switched in $\sim$50 ps,[37] we can also assume that with this ramp rate, the stress follows the voltage quasi-statically.

The minimum stress needed to switch the magnetization with $\sim$100% probability at 0 K is $\sim$5 MPa, but at 300 K, it

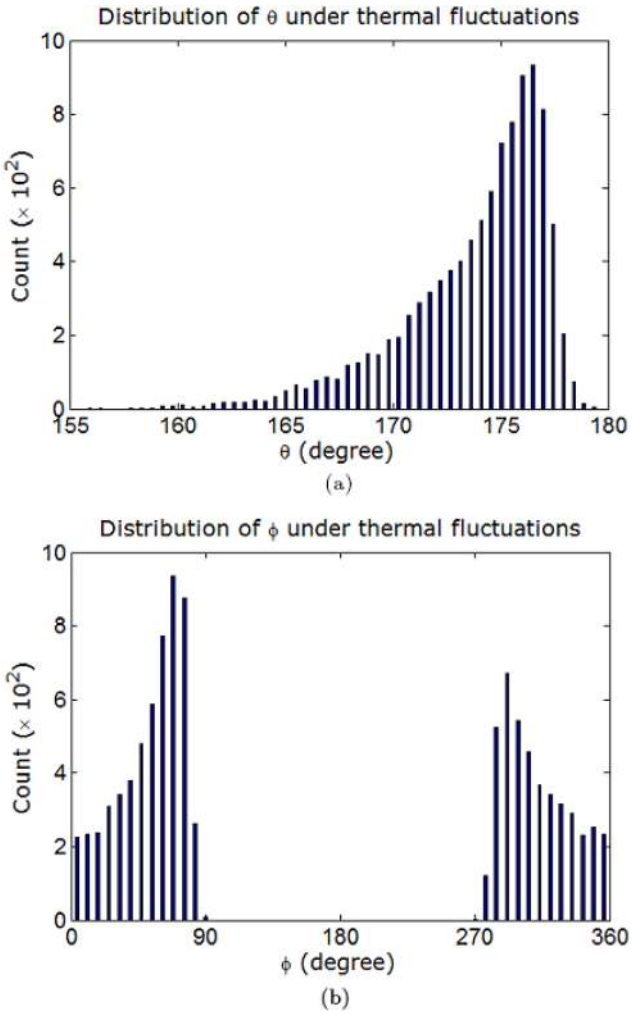

FIG. 2. Distribution of polar angle $\theta_{initial}$ and azimuthal angle $\phi_{initial}$ due to thermal fluctuations at room temperature (300 K) when a magnetic field of flux density 40 mT is applied along the out-of-plane hard axis (+x-direction). (a) Distribution of polar angle $\theta_{initial}$ at room temperature (300 K). The mean of the distribution is 173.7°, and the most likely value is 175.8°. (b) Distribution of the azimuthal angle $\phi_{initial}$ due to thermal fluctuations at room temperature (300 K). There are two distributions with peaks centered at ~65° and ~295°.

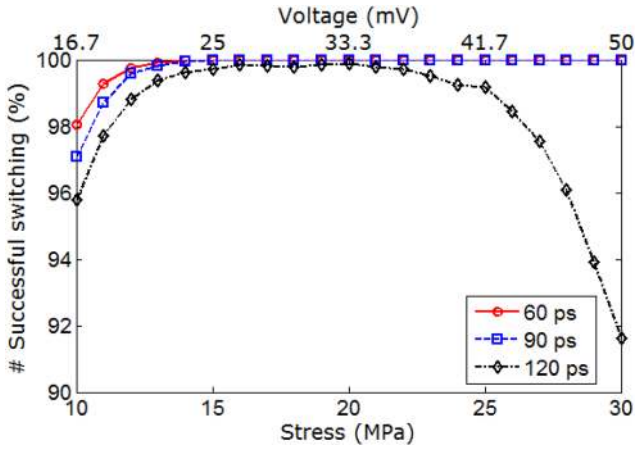

FIG. 3. Percentage of successful switching events among the simulated switching trajectories (or the switching probability) at room temperature in a Terfenol-D/PZT multiferroic nanomagnet versus (lower axis) stress (10–30 MPa) and (upper axis) voltage applied across the piezoelectric layer, for different ramp durations (60 ps, 90 ps, 120 ps). The stress at which switching becomes ~100% successful increases with ramp duration. For large ramp duration (120 ps) or slow ramp rate, ~100% switching probability is unachievable.

increases to ~14 MPa for 60 ps ramp duration and ~17 MPa for 90 ps ramp duration. At low stress levels, the switching probability increases with stress, regardless of the ramp rate. This happens because a higher stress can more effectively counter the detrimental effects of thermal fluctuations when the magnetization vector reaches the $x-y$ plane, and hence increases the success rate of switching. This feature is independent of the ramp rate.

Once the magnetization vector crosses the $x-y$ plane (i.e., in the second half of switching), the stress must be withdrawn as soon as possible. This is because the stress, initially applied to cause switching, forces the energy minimum to remain at $\theta = 90°$, instead of $\theta = 0°$, which will make the magnetization linger around $\theta = 90°$ instead of rotating towards the desired location at $\theta \simeq 0°$. This is why stress must be removed or reversed immediately upon crossing the $x-y$ plane so that the energy minimum quickly moves to $\theta = 0°, 180°$, and the magnetization vector rotates towards $\theta = 0°$. If the removal rate is fast, then the success probability remains high since the harmful stress does not stay active long enough to cause significant backtracking of the magnetization vector towards $\theta = 90°$. However, if the ramp rate is too slow, then significant backtracking occurs whereupon the magnetization vector returns to the $x-y$ plane and thermal torques can subsequently kick it to the starting position at $\theta \simeq 180°$, causing switching failure. That is why the switching probability drops with decreasing ramp rate.

The same effect also explains the non-monotonic stress dependence of the switching probability when the ramp rate is slow. During the first half of the switching, when θ is in the quadrant [180°, 90°], a higher stress is helpful since it provides a larger torque to move towards the $x-y$ plane, but during the second half, when θ is in the quadrant [90°, 0°], a higher stress is harmful since it increases the chance of backtracking, particularly when the ramp-down rate is slow. These two counteracting effects are the reason for the non-monotonic dependence of the success probability on stress in the case of the slowest ramp rate.

Fig. 4 shows the thermally averaged switching delay versus stress (as well as voltage applied across the piezoelectric layer) for different ramp durations. Only successful switching events are counted here since the switching delay will be infinity for an unsuccessful event. For a given stress, decreasing the ramp duration (or increasing the ramp rate) decreases the switching delay because the stress reaches its maximum value quicker and hence switches the magnetization faster. For ramp durations of 60 ps and 90 ps, the switching delay decreases with increasing stress since the torque, which rotates the magnetization, increases when stress increases. However, for 120 ps ramp duration, the dependence is non-monotonic, because of the same reasons that caused the non-monotonicity in Fig. 3. Too high a stress is harmful during the second half of the switching since it increases the chances of backtracking. Even if backtracking can be overcome and successful switching ultimately takes place, temporary backtracking still increases the switching delay.

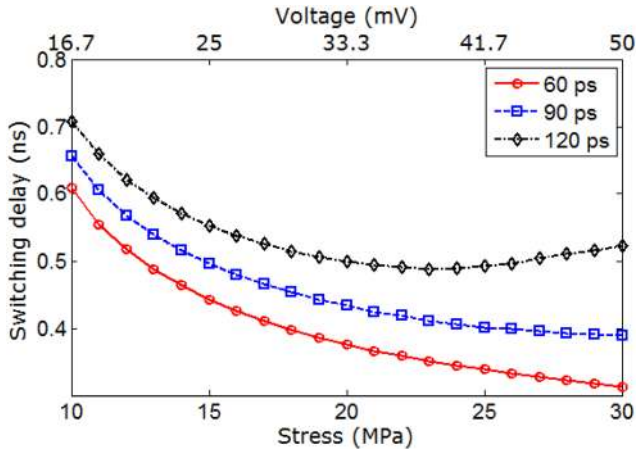

FIG. 4. The thermal mean of the switching delay (at 300 K) versus (lower axis) stress (10–30 MPa) and (upper axis) voltage applied across the piezoelectric layer, for different ramp durations (60 ps, 90 ps, 120 ps). Switching may fail at low stress levels and also at high stress levels for long ramp durations. Failed attempts are excluded when computing the mean.

Fig. 5 shows the standard deviation in switching delay versus stress (as well as voltage applied across the piezoelectric layer) for 60 ps ramp duration. At higher values of stress, the torque due to stress dominates over the random thermal torque that causes the spread in the switching delay. That makes the distribution more peaked as we increase the stress.

Fig. 6 shows the thermal mean of the total energy dissipated to switch the magnetization as a function of stress and voltage across the piezoelectric layer for different ramp durations. The average power dissipation (E_{total}/τ) increases with stress for a given ramp duration and decreases with increasing ramp duration for a given stress. More stress requires more "CV^2" dissipation and also more internal dissipation because it results in a higher torque. Slower switching decreases the power dissipation since it makes the switching more adiabatic. However, the switching delay curves show the opposite trend (see Fig. 4). At a lower ramp rate (higher ramp duration), the average power dissipation E_{total}/τ is

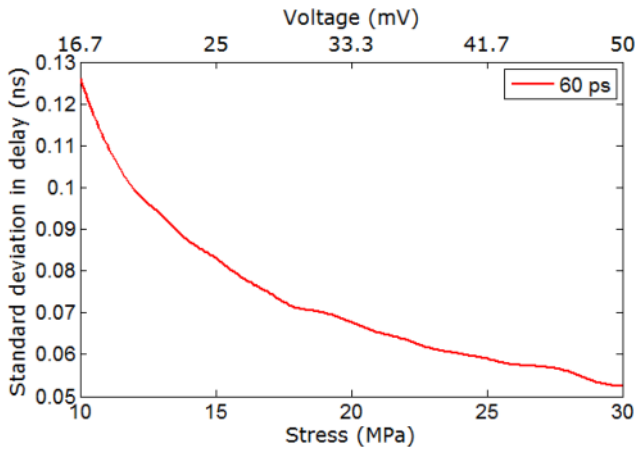

FIG. 5. The standard deviations in switching delay versus (lower axis) stress (10-30 MPa) and (upper axis) voltage applied across the piezoelectric layer for 60 ps ramp duration at 300 K. We consider only the successful switching events in determining the standard deviations. The standard deviations in switching delay for other ramp durations are of similar magnitudes and show similar trends.

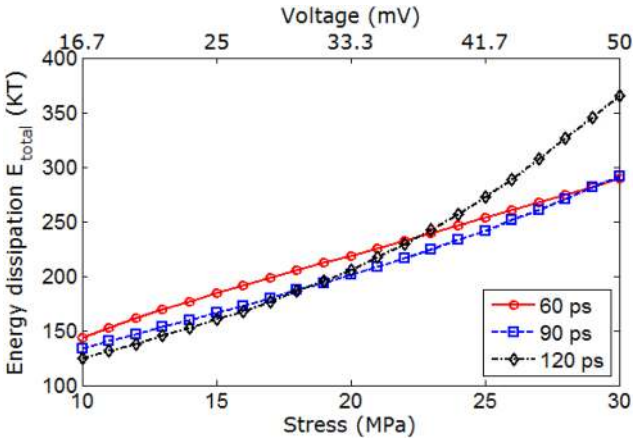

FIG. 6. Thermal mean of the total energy dissipation versus (lower axis) stress (10–30 MPa) and (upper axis) voltage across the piezoelectric layer for different ramp durations (60 ps, 90 ps, 120 ps). Once again, failed switching attempts are excluded when computing the mean.

always smaller than that of a higher ramp rate, but the switching delay does not decrease as fast as with higher values of stress (in fact switching delay may increase for higher ramp duration), which is why the energy dissipation curves in Fig. 6 exhibit the cross-overs.

Fig. 7 shows the "CV^2" energy dissipation in the switching circuitry versus stress and the voltage applied across the PZT layer. Increasing stress requires increasing the voltage V, which is why the "CV^2" energy dissipation increases rapidly with stress. This dissipation however is a small fraction of the total energy dissipation (<15%), since a very small voltage is required to switch the magnetization of a multiferroic nanomagnet with stress. The "CV^2" dissipation decreases when the ramp duration increases because then the switching becomes more "adiabatic" and hence less dissipative. This component of the energy dissipation would have been several orders of magnitude higher had we switched the magnetization with an external magnetic field[38] or spin-transfer torque.[17]

Fig. 8 shows the delay and energy distributions in the presence of room-temperature thermal fluctuations for

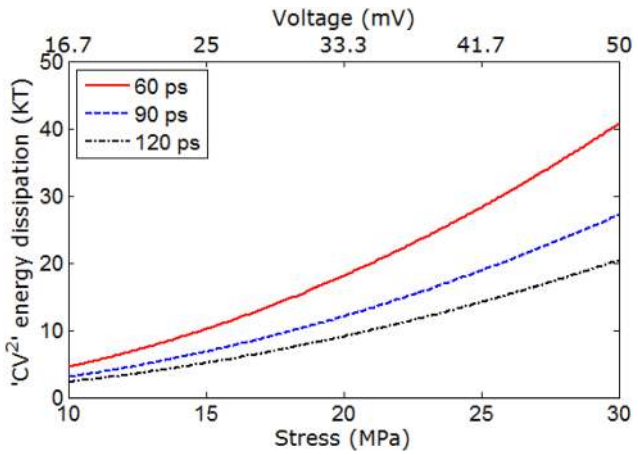

FIG. 7. The "CV^2" energy dissipation in the external circuit as a function of (lower axis) stress and (upper axis) voltage applied across the PZT layer for different ramp durations. The dependence on voltage is not exactly quadratic since the voltage is not applied abruptly, but instead ramped up gradually and linearly in time.

15 MPa stress and 60 ps ramp duration. The high-delay tail in Fig. 8(a) is associated with those switching trajectories that start very close to $\theta = 180^\circ$ which is a stagnation point. In such trajectories, the starting torque is vanishingly small, which makes the switching sluggish at the beginning. During this time, switching also becomes susceptible to backtracking because of thermal fluctuations, which increases the delay further. Nonetheless, out of 10000 simulations of switching trajectories, there was not a single one where the delay exceeded 1 ns, showing that the probability of that happening is less than 0.01%. The product of the average power dissipation and the switching delay, i.e., the energy dissipation, shows a similar behavior as plotted in Fig. 8(b).

Fig. 9 shows two examples of switching dynamics when the applied stress is 10 MPa and the ramp duration is 60 ps. In Fig. 9(a), magnetization switches successfully. Thermal fluctuations cause the ripples because of temporary backtracking but θ switches from $\sim 180^\circ$ to $\sim 0^\circ$ finally. Note that despite appearances, ϕ is not changing discretely. When it crosses 360°, it re-enters the quadrant $[0^\circ, 90^\circ]$, which is why it appears as if there is a discrete jump in the value of ϕ in Fig. 9. On the other hand, Fig. 9(b) shows a failed switching dynamics. Here, the magnetization backtracks towards

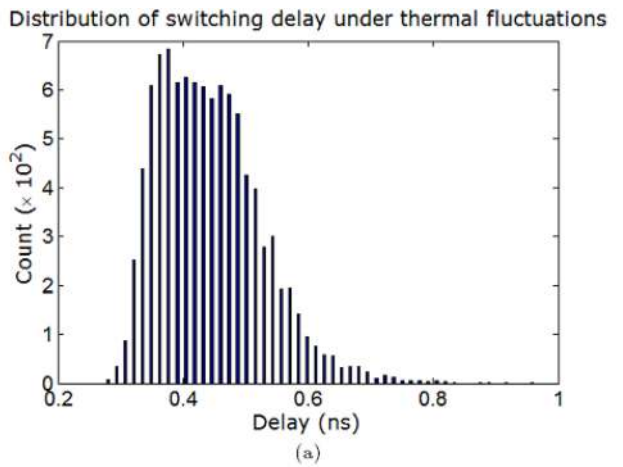

FIG. 8. Delay and energy distributions for 15 MPa applied stress and 60 ps ramp duration at room temperature (300 K). (a) Distribution of the switching delay. The mean and standard deviation of the distribution are 0.44 ns and 83 ps, respectively. (b) Distribution of energy dissipation. The mean and standard deviation of the distribution are 184 kT and 15.5 kT at room temperature, respectively.

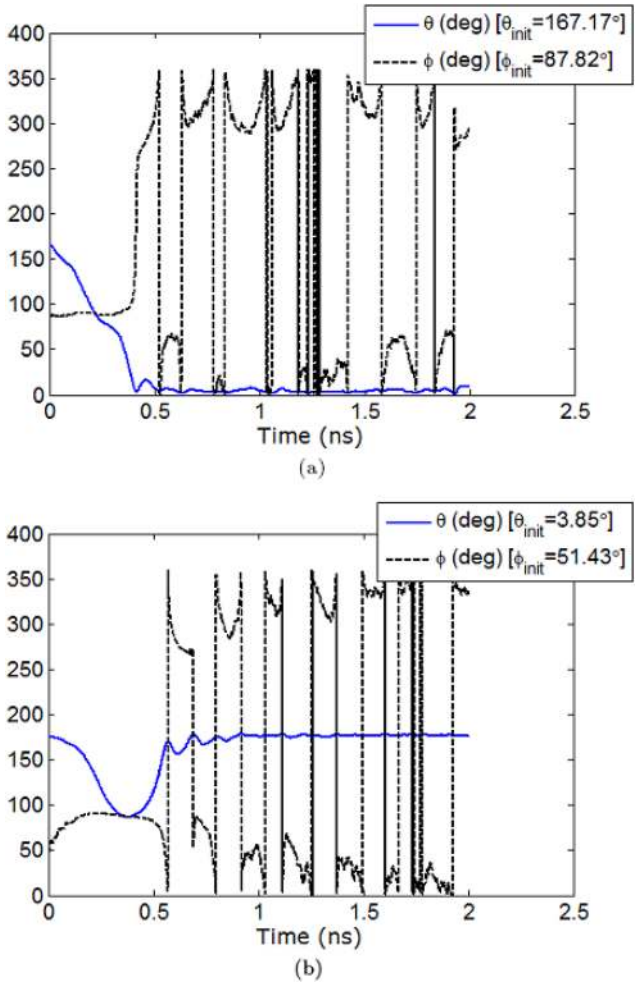

FIG. 9. Temporal evolution of the polar angle $\theta(t)$ and azimuthal angle $\phi(t)$ for 10 MPa applied stress and 60 ps ramp duration. Simulations are carried out for room temperature (300 K). (a) Magnetization switches successfully. (b) Magnetization fails to switch and backtracks towards the initial state.

$\theta = 180^\circ$ and settles close to that location, thus failing in its attempt to switch. This happened because of the coupled θ-ϕ dynamics that resulted in a misdirected torque when the magnetization reached the $x - y$ plane. This kind of dynamics has been explained in Ref. 24.

IV. CONCLUSIONS

We have theoretically investigated stress-induced switching of multiferroic nanomagnets in the presence of thermal fluctuations. The room-temperature thermal average of the energy dissipation is as small as $\sim 200\ kT$ while the thermal average of the switching delay is ~ 0.5 ns with a standard deviation less than 0.1 ns. This makes strain-switched multiferroic nanomagnets very attractive platforms for implementing non-volatile memory and logic systems because they are minimally dissipative while being adequately fast. Our results also show that a certain critical stress is required to switch with $\sim 100\%$ probability in the presence of thermal noise. The value of this critical stress increases with decreasing ramp rate until the ramp rate becomes so slow that $\sim 100\%$ switching probability becomes unachievable. Thus, a faster ramp rate is beneficial. The energy

dissipations and switching delays are roughly independent of ramp rate if switching is always performed with the critical stress.

ACKNOWLEDGMENTS

This work was supported by the U.S. National Science Foundation under Nanoelectronics for 2020 and Beyond (NEB) grant ECCS-1124714 and by the Semiconductor Research Corporation under the Nanoelectronics Research Initiative (NRI) Task 2203.001.

[1]N. A. Spaldin and M. Fiebig, Science **309**, 391 (2005).
[2]W. Eerenstein, N. D. Mathur, and J. F. Scott, Nature **442**, 759 (2006).
[3]C. W. Nan, M. I. Bichurin, S. Dong, D. Viehland, and G. Srinivasan, J. Appl. Phys. **103**, 031101 (2008).
[4]A. Khitun, D. E. Nikonov, and K. L. Wang, J. Appl. Phys. **106**, 123909 (2009).
[5]S. A. Wolf, J. Lu, M. R. Stan, E. Chen, and D. M. Treger, Proc. IEEE **98**, 2155 (2010).
[6]K. Roy, S. Bandyopadhyay, and J. Atulasimha, Appl. Phys. Lett. **99**, 063108 (2011).
[7]K. Roy, S. Bandyopadhyay, and J. Atulasimha, Phys. Rev. B **83**, 224412 (2011).
[8]J. Atulasimha and S. Bandyopadhyay, Appl. Phys. Lett. **97**, 173105 (2010).
[9]M. S. Fashami, K. Roy, J. Atulasimha, and S. Bandyopadhyay, Nanotechnology **22**, 155201 (2011).
[10]N. D′Souza, J. Atulasimha, and S. Bandyopadhyay, J. Phys. D: Appl. Phys. **44**, 265001 (2011).
[11]T. Brintlinger, S. H. Lim, K. H. Baloch, P. Alexander, Y. Qi, J. Barry, J. Melngailis, L. Salamanca-Riba, I. Takeuchi, and J. Cumings, Nano Lett. **10**, 1219 (2010).
[12]T. K. Chung, S. Keller, and G. P. Carman, Appl. Phys. Lett. **94**, 132501 (2009).
[13]T. Wu, A. Bur, K. Wong, P. Zhao, C. S. Lynch, P. K. Amiri, K. L. Wang, and G. P. Carman, Appl. Phys. Lett. **98**, 262504 (2011).
[14]N. Tiercelin, Y. Dusch, A. Klimov, S. Giordano, V. Preobrazhensky, and P. Pernod, Appl. Phys. Lett. **99**, 192507 (2011).
[15]T. L. Gilbert, IEEE Trans. Magn. **40**, 3443 (2004).
[16]W. F. Brown, Phys. Rev. **130**, 1677 (1963).
[17]J. Z. Sun, Phys. Rev. B **62**, 570 (2000).
[18]S. Mark, P. Durrenfeld, K. Pappert, L. Ebel, K. Brunner, C. Gould, and L. W. Molenkamp, Phys. Rev. Lett. **106**, 57204 (2011).
[19]B. Behin-Aein, D. Datta, S. Salahuddin, and S. Datta, Nat. Nanotechnol. **5**, 266 (2010).
[20]S. Chikazumi, *Physics of Magnetism* (Wiley New York, 1964).
[21]M. Beleggia, M. D. Graef, Y. T. Millev, D. A. Goode, and G. E. Rowlands, J. Phys. D: Appl. Phys. **38**, 3333 (2005).
[22]R. P. Cowburn, D. K. Koltsov, A. O. Adeyeye, M. E. Welland, and D. M. Tricker, Phys. Rev. Lett. **83**, 1042 (1999).
[23]G. Brown, M. A. Novotny, and P. A. Rikvold, Phys. Rev. B **64**, 134422 (2001).
[24]K. Roy, S. Bandyopadhyay, and J. Atulasimha, e-print arXiv:1111.5390. Available at http://arxiv.org/abs/1111.5390.
[25]A. Brataas, G. E. W. Bauer, and P. J. Kelly, Phys. Rep. **427**, 157 (2006).
[26]Z. Z. Sun and X. R. Wang, Phys. Rev. B **73**, 092416 (2006).
[27]Z. Z. Sun and X. R. Wang, Phys. Rev. B **71**, 174430 (2005).
[28]B. Behin-Aein, S. Salahuddin, and S. Datta, IEEE Trans. Nanotechnol. **8**, 505 (2009).
[29]L. B. Kish, Phys. Lett. A **305**, 144 (2002).
[30]R. Abbundi and A. E. Clark, IEEE Trans. Magn. **13**, 1519 (1977).
[31]K. Ried, M. Schnell, F. Schatz, M. Hirscher, B. Ludescher, W. Sigle, and H. Kronmüller, Phys. Status Solidi A **167**, 195 (1998).
[32]R. Kellogg and A. Flatau, J. Intell. Mater. Syst. Struct. **19**, 583 (2008).
[33]See http://www.allmeasures.com/Formulae/static/materials/ for material parameters.
[34]M. Lisca, L. Pintilie, M. Alexe, and C. M. Teodorescu, Appl. Surf. Sci. **252**, 4549 (2006).
[35]A. J. Masys, W. Ren, G. Yang, and B. K. Mukherjee, J. Appl. Phys. **94**, 1155 (2003).
[36]See http://www.memsnet.org/material/leadzirconatetitanatepzt/ for d_{31} coefficient of PZT.
[37]J. Li, B. Nagaraj, H. Liang, W. Cao, C. Lee, and R. Ramesh, Appl. Phys. Lett. **84**, 1174 (2004).
[38]M. T. Alam, M. J. Siddiq, G. H. Bernstein, M. T. Niemier, W. Porod, and X. S. Hu, IEEE Trans. Nanotechnol. **9**, 348 (2010).